Energy-Efficient UAV Deployment and IoT Device Association in Fixed-Wing Multi-UAV Networks

Jen-Hao Chiu[†], Yung-Ching Kuo[†], Jang-Ping Sheu[†‡], and Y.-W. Peter Hong[‡⋆]

[†]Department of Computer Science, National Tsing Hua University, Taiwan
[‡]Insititute of Communications Engineering, National Tsing Hua University, Taiwan
[⋆]MOST Joint Research Center for AI Technology and AII Vista Healthcare, Taiwan
Emails: {q910553,cludbuster}@gmail.com, {sheujp@cs, ywhong@ee}.nthu.edu.tw

GLOBECOM 2020 - 2020 IEEE Global Communications Conference | 978-1-7281-8298-8/20/$31.00 ©2020 IEEE | DOI: 10.1109/GLOBECOM42002.2020.9322292

***Abstract*—This work examines the deployment of multiple fixed-wing unmanned aerial vehicles (UAVs) for data-gathering from ground IoT devices, and the corresponding device association policy. Each UAV is assumed to hover above its associated devices following a circular trajectory. The device association and the UAVs' trajectory centers and radii are jointly optimized to maximize the energy-savings relative to a constant transmission power scheme. Given the trajectory centers and radii, the device association problem is modeled as a multiple 0-1 knapsack problem, taking into consideration the load demands of different devices as well as UAVs' service capacities. A two-stage maximum energy-saving device association policy is proposed, where each UAV first solves a single knapsack problem based on all connectable devices, and then resolves conflict with others by a maximum profit assignment. Moreover, given the device association, the UAVs' trajectory centers and radii are optimized by an iterative load-balancing algorithm, where the trajectory centers are chosen as a load-dependent weighted sum of the associated devices' locations. The device association and the UAV deployment are optimized in turn until convergence. Simulation results show that our proposed schemes outperform candidate algorithms in terms of the total energy-savings of IoT devices.**

I. Introduction

The use of unmanned aerial vehicles (UAVs) as flying wireless communication platforms has received much attention in recent years due to UAVs high mobility and deployment flexibility [1], [2]. In cellular applications, UAVs have been adopted as temporary base-stations (BSs) for data-offloading [3] and disaster recovery [4], and as relays for coverage extension in remote areas [5], [6]. In internet-of-things (IoT) or wireless sensor networks (WSN), UAVs have also been used as mobile aggregators or sink nodes for efficient data collection [7], [8]. Compared to the use of ground BSs for data collection, UAVs can be moved dynamically toward IoT devices to reduce their uplink energy consumption. The altitude of UAVs may also be adjusted to increase the probability of line-of-sight (LoS). In this case, the UAVs' 3D placement or trajectory design, and the IoT devices power control and association must be carefully designed in order to fully exploit these advantages.

Specifically, the use of UAVs for data collection in IoT has been examined in the literature for cases with single [9]–[11] and multiple UAVs [12]–[14], respectively. In [9], the propulsion energy of a fixed-wing UAV was derived, and an energy-efficient trajectory design was proposed by maximizing the total communicated information bits per unit energy consumption by the UAV. In [10], the UAV's trajectory and the sensors' wake-up schedule are jointly determined to minimize the maximum energy consumption of all sensors. In [11], the UAV's trajectory was designed to minimize the flight time while allowing each sensor to upload a certain amount of data with limited energy consumption. Moreover, in [12], the joint optimization of multiple rotary-wing UAVs' 3D placement, device association, and uplink power control was considered to minimize the transmission power of ground devices. In [13], a similar problem was examined but with additional consideration on the UAVs' limited hover times. In [14], the UAV deployment, device association, and uplink resource allocation were jointly optimized for multiple rotary-wing UAVs with the goal of maximizing the lifetime of ground devices. Different from [12]–[14], our work considers the deployment of multiple fixed-wing UAVs and the association of devices to these constantly-moving UAVs.

This work examines the deployment of multiple fixed-wing UAVs, and the association of IoT devices to maximize the total uplink energy-savings of the devices. To stay afloat, each fixed-wing UAV is assumed to follow a periodic circular flight trajectory above its associated devices. Given the UAVs' trajectory centers and radii, the device association problem is modeled as a 0-1 multiple knapsack problem with assign restrictions (MKPAR) [15], [16], which is known to be NP-hard. We propose a two-stage maximum energy-saving (MES) device association policy, where each UAV first solves a single knapsack problem locally by considering all connectable devices, and then resolves conflict with other UAVs using a maximum profit assignment scheme. Moreover, given the device association, the UAVs' trajectory centers and radii are optimized using an iterative load-balancing (ILB) algorithm, where the centers are chosen as a load-dependent weighted sum of its associated devices' locations. The device association and the UAV deployment are optimized in turn until convergence. Simulation results are provided to demonstrate the effectiveness of the proposed scheme. It is worthwhile to note that, while this work focuses on the uplink transmission from the devices to the UAVs, the data collected by the UAVs

This work is supported in part by Ministry of Science and Technology, Taiwan, under grant 108-2634-F-007-004 and 109-2634-F-007-015.

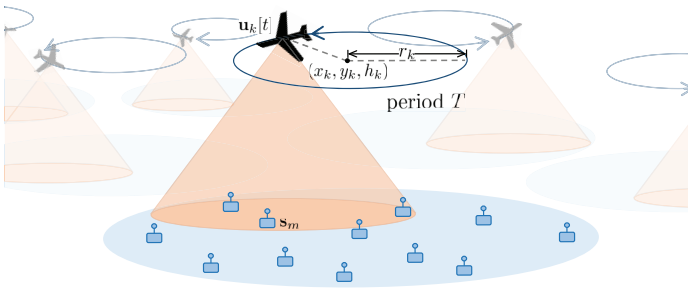

Fig. 1. Illustration of multiple fixed-wing UAVs.

can be further sent to a central data-gathering node using, e.g., multi-hop transmissions, as examined in [17].

II. System Model and Problem Formulation

Let us consider an IoT network with M devices deployed on the ground over a bounded region of interest, and K fixed-wing UAVs circling above their respective coverage regions to gather data from the ground devices, as illustrated in Fig. 1. The devices and UAVs are denoted by the sets $\mathcal{M} = \{1, \ldots, M\}$ and $\mathcal{K} = \{1, \ldots, K\}$, respectively. The locations of ground devices are assumed to be fixed whereas those of fixed-wing UAVs vary constantly over time. Therefore, we denote the location of ground device $m \in \mathcal{M}$ by the 3D coordinates $\mathbf{s}_m = (s_{m,1}, s_{m,2}, s_{m,3})$, where the altitude $s_{m,3}$ is assumed to be 0, and the location of UAV $k \in \mathcal{K}$ at time t by $\mathbf{u}_k[t] = (u_{k,1}[t], u_{k,2}[t], u_{k,3}[t])$. Different from rotary-wing UAVs [1], fixed-wing UAVs must be constantly moving in order to stay afloat. In our case, we assume that each UAV follows a circular flight trajectory with period T above their respective coverage region. Hence, the location of UAV k at time t can be expressed as

$$\mathbf{u}_k[t] = (x_k + r_k \cos(2\pi t/T),\ y_k + r_k \sin(2\pi t/T),\ h_k), \quad (1)$$

where (x_k, y_k) represents the two-dimensional center coordinates of the circular trajectory of UAV k on the horizontal plane, h_k is the altitude, and r_k is the radius.

We consider an uplink scenario in which each IoT device is associated with at most one UAV, and the transmissions of IoT devices occur over orthogonal channels. In particular, the IoT devices associated with the same UAV are scheduled to transmit in orthogonal time slots whereas those associated with different UAVs transmit over different frequency bands. The association between devices and UAVs are described by the binary association variables $a_{m,k}$, for $m = 1, \ldots, M$ and $k = 1, \ldots, K$, where $a_{m,k} = 1$ if device m is associated with UAV k and $a_{m,k} = 0$, otherwise. Moreover, we have $\sum_{k=1}^{K} a_{m,k} \leq 1$, for all m. The traffic demand of device m is given by λ_m in terms of the number of bits per flight cycle T, and the maximum number of bits that UAV k can receive over time T (i.e., the capacity limit of UAV k) is given by μ_k. In this case, device m must occupy λ_m/μ_k fraction of the time available for transmission to UAV k in each flight cycle (i.e., $\frac{\lambda_m}{\mu_k} T$). Moreover, we say that the transmission from device m to UAV k at time t is successful if the receive SNR at this time exceeds the threshold γ_k.

A. Ground-to-Air Path Loss Model

Let $P_m[t] \in [0, P_{\max}]$ be the transmission power of device m at time t, where $P_{\max}$ is the maximum transmission power of each device. Then, the signal-to-noise ratio (SNR) between device m and UAV k at time t can be written as

$$\mathrm{SNR}_m(\mathbf{u}_k[t]) \triangleq \frac{P_m[t]}{\overline{\mathrm{PL}}_m(\mathbf{u}_k[t])\sigma_k^2}, \quad (2)$$

where $\overline{\mathrm{PL}}_m(\mathbf{u}_k[t])$ is the path loss between device m and UAV k, and σ_k^2 is the noise variance at UAV k. Following the ground-to-air path loss model in [18], which takes into consideration the probability of line-of-sight (LoS) between the ground device and the UAV based on their relative locations, the path loss can be expressed (in dB) as

$$\begin{aligned}\left(\overline{\mathrm{PL}}_m(\mathbf{u}_k[t])\right)_{\mathrm{dB}} &= 10\log_{10}\left(\frac{4\pi f_c}{c}\right)^2 + 10\log_{10}\|\mathbf{s}_m - \mathbf{u}_k[t]\|^\alpha \\ &\quad + \eta_{\mathrm{LoS}}\,\rho_{m,\mathrm{LoS}}(\mathbf{u}_k[t]) + \eta_{\mathrm{NLoS}}[1 - \rho_{m,\mathrm{LoS}}(\mathbf{u}_k[t])] \quad (3)\end{aligned}$$

where f_c is the carrier frequency, c is the speed of light, α is the path loss coefficient, η_{LoS} and η_{NLoS} are the excessive path loss coefficients corresponding to LoS and NLoS links, respectively, and $\rho_{m,\mathrm{LoS}}(\mathbf{u}_k[t])$ is the probability of LoS between device m and UAV k at time t. The LoS probability can be approximated as [18]

$$\rho_{m,\mathrm{LoS}}(\mathbf{u}_k[t]) = \frac{1}{1 + \psi \exp\{-\beta[\theta_m(\mathbf{u}_k[t]) - \psi]\}}, \quad (4)$$

where ψ and β are parameters depending on the environment (e.g., rural or urban) and $\theta_m(\mathbf{u}_k[t]) = \frac{180}{\pi}\sin^{-1}(h_k/\|\mathbf{s}_m - \mathbf{u}_k[t]\|)$ is the elevation angle between device m and UAV k at time t. Notice from (4) that, by increasing the flight altitude of UAV k (i.e., h_k), the elevation angle (and, thus, the LoS probability) between device m and UAV k increases, but the distance (and, thus, the signal decay) also increases. Hence, the flight altitudes of the UAVs must be carefully chosen in order to best exploit the trade-off between the LoS probability and the signal decay over distance.

B. Problem Formulation

The main objective of this work is to determine the UAVs' locations (which are determined by their 2D center coordinates (x_k, y_k), height h_k, and radius r_k, for all k), and the device association $\{a_{m,k}, \forall m, k\}$ to maximize the energy-savings (and, thus, reduce the energy consumption) of the ground IoT devices. To focus on the above issue, we consider an ideal scheduling where each IoT device is assumed to be able to transmit when its associated UAV arrives at its closest point in the flight trajectory. In this case, the distance between device m and UAV k at the closest point is given by

$$\min_{t\in[0,T]} \|\mathbf{s}_m - \mathbf{u}_k[t]\| = \sqrt{\|(s_{m,1} - x_k, s_{m,2} - y_k)\| - r_k)^2 + h_k^2}$$

and, thus, the path loss between device m and UAV k can be approximated as

$$\begin{aligned}\left(\overline{\mathrm{PL}}_m(\mathbf{u}_k[t])\right)_{\mathrm{dB}} &\approx \left(\overline{\mathrm{PL}}_m(x_k, y_k, h_k, r_k)\right)_{\mathrm{dB}} \triangleq 10\log_{10}\frac{4\pi f_c}{c} \\ &+ 10\log_{10}[(\|(s_{m,1}-x_k, s_{m,2}-y_k)\|-r_k)^2 + h_k^2]^{\frac{\alpha}{2}} \\ &+ \eta_{\mathrm{NLoS}} + \frac{\eta_{\mathrm{LoS}}-\eta_{\mathrm{NLoS}}}{1+\psi\exp\{-\beta[\theta_m(x_k,y_k,h_k,r_k)-\psi]\}} \end{aligned} \tag{5}$$

where

$$\begin{aligned}&\theta_m(x_k, y_k, h_k, r_k) \triangleq \\ &\frac{180}{\pi}\sin^{-1}\frac{h_k}{\sqrt{(\|(s_{m,1}-x_k, s_{m,2}-y_k)\|-r_k)^2+h_k^2}}\end{aligned} \tag{6}$$

is the elevation angle at the closest point. Notice that the path loss no longer depends on the time index t and, thus, the transmission power P_m can be fixed as well. The design of scheduling policies that can ensure minimum transmission distances between the devices and UAVs is beyond the scope of the current work, but will be investigated in future studies.

The proposed UAV deployment and device association problem can thus be formulated as

$$\max_{\substack{x_k,y_k,h_k,r_k,\\ a_{m,k},P_m,\forall m,k}} \quad \sum_{k=1}^{K}\sum_{m=1}^{M} a_{m,k}\frac{\lambda_m}{\mu_k}T(P_{\max}-P_m), \tag{7a}$$

$$\text{subject to} \quad \sum_{k=1}^{K} a_{m,k} \le 1,\ a_{m,k}\in\{0,1\}, \tag{7b}$$

$$\sum_{m=1}^{M}\lambda_m a_{m,k} \le \mu_k, \tag{7c}$$

$$\frac{P_m}{\overline{\mathrm{PL}}_m(x_k,y_k,h_k,r_k)\sigma_k^2} \ge a_{m,k}\gamma_k, \tag{7d}$$

$$h_{\min}\le h_k\le h_{\max},\ r_{\min}\le r_k\le r_{\max} \tag{7e}$$

$$0<P_m\le P_{\max},\ \forall m,k. \tag{7f}$$

Notice that the objective represents the total energy-savings that can be experienced by the IoT devices compared to transmitting at maximum power since $\lambda_m T/\mu_k$ represents the time scheduled for device m's transmission to UAV k. The constraint in (7b) ensures that each device is associated with at most one UAV, (7c) ensures that the scheduled transmissions are within the capacity limit of each UAV, and (7d) ensures that the transmissions of associated devices are successful. The remaining constraints provide upper and lower bounds to the flight altitude, radius, and transmission power.

In the following sections, we propose to solve the device association and the UAV deployment problems in an alternating fashion, where one problem is solved while the solution of the other is fixed. In particular, given the UAVs' trajectory centers and radii, the device association problem is first modelled as a 0-1 multiple knapsack problem with assignment restrictions (MKPAR) [15] and an approximate algorithm is proposed to solve the problem. Then, given the device association, the UAVs' locations are then determined using a weighted averaging of the associated devices' locations.

III. Device Association as a 0-1 Multiple Knapsack Problem with Assignment Restrictions

In this section, we examine the device association problem (i.e., the optimization over the binary association variables $\{a_{k,m}, \forall k, m\}$) for fixed UAVs' trajectory centers and radii (i.e., $\{x_k, y_k, h_k, r_k, \forall k\}$). We show that the problem can be modeled as a 0-1 MKPAR problem [15], [16] and propose an approximate algorithm to solve it. The proposed algorithm aims to maximize the IoT devices' energy-savings and, thus, is referred to as the maximum energy-savings (MES) device association algorithm.

Specifically, given the trajectory centers and radii (i.e., $\{x_k, y_k, h_k, r_k, \forall k\}$), the problem in (7) reduces to

$$\max_{a_{m,k},P_m,\forall m,k} \quad \sum_{k=1}^{K}\sum_{m=1}^{M} a_{m,k}\frac{\lambda_m}{\mu_k}T(P_{\max}-P_m), \tag{8a}$$

$$\text{subject to} \quad \sum_{k=1}^{K} a_{m,k} \le 1,\ a_{m,k}\in\{0,1\}, \tag{8b}$$

$$\sum_{m=1}^{M}\lambda_m a_{m,k} \le \mu_k, \tag{8c}$$

$$a_{m,k}\tilde{\gamma}_{m,k} \le P_m \le P_{\max}, \tag{8d}$$

where $\tilde{\gamma}_{m,k} \triangleq \gamma_k\sigma_k^2\overline{\mathrm{PL}}_m(x_k,y_k,h_k,r_k)$ is the minimum required transmission power of device m when it is associated with UAV k. This problem can be viewed as a 0-1 MKPAR problem where each UAV, say UAV k, is a knapsack with capacity μ_k, and each device, say device m, is an item with weight λ_m. The capacity of a knapsack represents the maximum total weight of items that it can accommodate. Here, the assignment of item m to knapsack k is said to yield profit $\frac{\lambda_m}{\mu_k}T(P_{\max}-\tilde{\gamma}_{m,k})$, which represents the energy-saving of device m per flight cycle. However, to satisfy the constraint in (8d), the assignment to UAV k in this case must be restricted to the set $\mathcal{M}_k \triangleq \{m\in\mathcal{M} : \tilde{\gamma}_{m,k} < P_{\max}\}$. Consequently, the device association problem in (8) becomes equivalent to the profit-maximization problem in MKPAR.

To solve the MKPAR problem, we propose an approximate algorithm that involves solving the basic 0-1 single knapsack problem [16] in parallel for all UAVs followed by a profit-based reassignment policy to resolve conflict among UAVs. The algorithm can be summarized into two stages.

Stage 1 (0-1 Single Knapsack Problem):

In Stage 1, each UAV aims to solve the basic 0-1 single knapsack problem individually without consideration of other UAVs. In particular, each UAV, say UAV k, seeks to find the set of devices that it hopes to be associated with, i.e., the set

$$\mathcal{A}_k^* = \underset{\mathcal{A}_k\subset\mathcal{M}_k:\sum_{m\in\mathcal{A}_k}\lambda_m\le\mu_k}{\arg\max} \sum_{m\in\mathcal{A}_k}\frac{\lambda_m}{\mu_k}T(P_{\max}-\tilde{\gamma}_{m,k}). \tag{9}$$

This problem can be solved using standard dynamic programming techniques [16]. However, at the end of this stage, the subsets $\{\mathcal{A}_k^*\}_{k=1}^K$ may overlap with each other and, thus, must be resolved in order to satisfy the association constraint in (8b).

Algorithm 1 MES Device Association Algorithm

Initialize: $a_{m,k}=0$, for all m and k, and $\mathcal{M}_k=\{m\in\mathcal{M}:\tilde{\gamma}_{m,k}<P_{\max}\}$.
while $\mu_k\geq\min_{m\in\mathcal{M}_k}\lambda_m$, for some k **do**
  for $k=1$ to K **do**
    Find $\mathcal{A}_k^*$ by (9) using dynamic programming.
  end for
  for $k=1$ to K **do**
    Update $a_{m,k}$ according to (24), for all $m\in\mathcal{M}_k$.
  end for
  Update $\mu_k\leftarrow\mu_k-\sum_{m\in\mathcal{M}_k}\lambda_m a_{m,k}$ and $\mathcal{M}_k\leftarrow\mathcal{M}_k\setminus\left\{m\in\mathcal{M}_k:\sum_{k'=1}^{K}a_{m,k'}=1\right\}$, for all k.
end while
return $\{a_{m,k},\forall m,k\}$

Stage 2 (Maximum Profit Assignment):

In Stage 2, the devices that are simultaneously chosen by more than one UAV are resolved by associating the device to the UAV that yields the maximum profit. That is, we set

$$a_{m,k}=\begin{cases}1, & \text{for } k=\underset{k':\,m\in\mathcal{A}_{k'}^*}{\arg\max}\ \frac{\lambda_m}{\mu_k}T(P_{\max}-\tilde{\gamma}_{m,k'}),\\ 0, & \text{otherwise,}\end{cases}\tag{10}$$

for all $m\in\mathcal{M}_k$ and for all k.

Notice that, after Stage 2, the capacity of certain UAVs may be released due to the maximum-profit assignment in case of conflict. Hence, to fully utilize the remaining capacity of the UAVs, we repeat the two stages again with the updated UAV capacities and sets of connectable devices, i.e.,

$$\mu_k\leftarrow\mu_k-\sum_{m\in\mathcal{M}_k}\lambda_m a_{m,k},\tag{11}$$

$$\mathcal{M}_k\leftarrow\mathcal{M}_k\setminus\left\{m\in\mathcal{M}_k:\sum_{k'=1}^{K}a_{m,k'}=1\right\},\tag{12}$$

for all k. The process is repeated until no further assignment is possible. The algorithm is summarized in Algorithm 1.

IV. Load-Balancing UAV Deployment and Flight Radius Adjustment

In this section, we examine the UAV deployment and radius adjustment policy for given device associations. In this case, the maximization problem in (7) can be decoupled into K parallel minimization subproblems, one for each UAV, i.e.,

$$\min_{x_k,y_k,h_k,r_k}\ \sum_{m=1}^{M}a_{m,k}\lambda_m\tilde{\gamma}_{m,k}(x_k,y_k,h_k,r_k),\tag{13a}$$

$$\text{subject to}\ \ h_{\min}\leq h_k\leq h_{\max},\tag{13b}$$

$$r_{\min}\leq r_k\leq r_{\max},\tag{13c}$$

for $k=1,\ldots,K$, where $\tilde{\gamma}_{m,k}(x_k,y_k,h_k,r_k)$ is expressed as a function of (x_k,y_k,h_k,r_k) to emphasize its dependence on these variables. Here, we propose to solve this problem by an approximate coordinate descent algorithm which leads to an insightful iterative load-balancing (ILB) procedure.

For notational simplicity, let us express the vector of optimizing parameters as $\boldsymbol{\phi}_k\triangleq(x_k,y_k,h_k,r_k)$. Then, by (5) and by removing the terms not relevant to m or $\boldsymbol{\phi}_k$, the objective function in (13) can be simplified as

$$J(\boldsymbol{\phi}_k)\triangleq\sum_{m=1}^{M}a_{m,k}\Psi_m(\boldsymbol{\phi}_k)\left[\left(\sqrt{(s_{m,1}-x_k)^2+(s_{m,2}-y_k)^2}-r_k\right)^2+h_k^2\right]\tag{14}$$

where $\Psi_m(\boldsymbol{\phi}_k)\triangleq\lambda_m 10^{\frac{(\eta_{\mathrm{LoS}}-\eta_{\mathrm{NLoS}})/10}{1+\psi\exp\{-\beta[\theta_m(x_k,y_k,h_k,r_k)-\psi]\}}}$. Suppose that $\boldsymbol{\phi}^{(\ell)}\triangleq(x_k^{(\ell)},y_k^{(\ell)},h_k^{(\ell)},r_k^{(\ell)})$ is the solution obtained in the ℓ-th iteration of the coordinate descent algorithm. Then, in iteration $\ell+1$, the variables x_k and y_k can be updated as

$$x_k^{(\ell+1)}=x_k^{(\ell)}-\eta\frac{\partial J(\boldsymbol{\phi}_k^{(\ell)})}{\partial x_k^{(\ell)}}\tag{15}$$

and

$$y_k^{(\ell+1)}=y_k^{(\ell)}-\eta\frac{\partial J(\boldsymbol{\phi}_k^{(\ell)})}{\partial y_k^{(\ell)}}.\tag{16}$$

In particular, the partial derivative with respect to x_k at point $x_k^{(\ell)}$ can be written as

$$\frac{\partial J(\boldsymbol{\phi}_k^{(\ell)})}{\partial x_k^{(\ell)}}=\sum_{m=1}^{M}a_{m,k}\Bigg\{-2\Psi_m(\boldsymbol{\phi}_k^{(\ell)})(s_{m,1}-x_k^{(\ell)})\cdot\left(1-\frac{r_k^{(\ell)}}{\sqrt{(s_{m,1}-x_k^{(\ell)})^2+(s_{m,2}-y_k^{(\ell)})^2}}\right)+\frac{\partial\Psi_m(\boldsymbol{\phi}_k^{(\ell)})}{\partial x_k^{(\ell)}}\cdot\left[\left(\sqrt{(s_{m,1}-x_k^{(\ell)})^2+(s_{m,2}-y_k^{(\ell)})^2}-r_k^{(\ell)}\right)^2+(h_k^{(\ell)})^2\right]\Bigg\}\tag{17}$$

Notice that, for h_k sufficiently large, small changes in the UAV's horizontal position would not have a significant impact on the elevation angle and, thus, we can assume that $\frac{\partial\Psi_m(\boldsymbol{\phi}_k)}{\partial x_k}$ is small and that the second term is negligible. In this case, the derivative can be approximated as

$$\frac{\partial J(\boldsymbol{\phi}_k^{(\ell)})}{\partial x_k^{(\ell)}}\approx-2\sum_{m=1}^{M}a_{m,k}\tilde{\Psi}_m(\boldsymbol{\phi}_k^{(\ell)})(s_{m,1}-x_k^{(\ell)})\tag{18}$$

where $\tilde{\Psi}_m(\boldsymbol{\phi}_k)\triangleq\Psi_m(\boldsymbol{\phi}_k)\left(1-\frac{r_k}{\sqrt{(s_{m,1}-x_k)^2+(s_{m,2}-y_k)^2}}\right)$. Then, the coordinate descent update of x_k in iteration $\ell+1$ can be approximated as

$$x_k^{(\ell+1)}\approx x_k^{(\ell)}+2\eta\sum_{m=1}^{M}a_{m,k}\tilde{\Psi}_m(\boldsymbol{\phi}_k^{(\ell)})(s_{m,1}-x_k^{(\ell)}).\tag{19}$$

Moreover, by choosing $\eta=\frac{\alpha}{2\eta\sum_{m'=1}^{M}a_{m',k}\tilde{\Psi}_{m'}(\boldsymbol{\phi}_k^{(\ell)})}$, we have

$$x_k^{(\ell+1)}\approx(1-\alpha)x_k^{(\ell)}+\alpha\tilde{x}_k^{(\ell+1)},\tag{20}$$

Algorithm 2 ILB UAV Deployment and Radius Adjustment Algorithm (for UAV k)

1: **Initialize:** Set $\ell = 0$ and the initial values of $(x_k^{(0)}, y_k^{(0)})$, $h_k^{(0)}$, and $r_k^{(0)}$ as UAV k's current position and radius.
2: **while** $\|\boldsymbol{\phi}_k^{(\ell+1)} - \boldsymbol{\phi}_k^{(\ell)}\| / \|\boldsymbol{\phi}_k^{(\ell)}\| > \epsilon$ **do**
3: Update the center coordinates as

$$x_k^{(\ell+1)} \approx (1-\alpha) x_k^{(\ell)} + \alpha \tilde{x}_k^{(\ell+1)},$$
$$y_k^{(\ell+1)} = (1-\alpha) y_k^{(\ell)} + \alpha \tilde{y}_k^{(\ell+1)},$$

where $\tilde{x}_k^{(\ell+1)}$ and $\tilde{y}_k^{(\ell+1)}$ are the load-balancing coordinates defined in (21) and (23), respectively.
4: Update $h_k^{(\ell+1)}$ and $r_k^{(\ell+1)}$, as in (24), by a two-dimensional line search.
5: **end while**

where

$$\tilde{x}_k^{(\ell+1)} \triangleq \sum_{m=1}^{M} \frac{a_{m,k} \tilde{\Psi}_m(\boldsymbol{\phi}_k^{(\ell)})}{\sum_{m'=1}^{M} a_{m',k} \tilde{\Psi}_{m'}(\boldsymbol{\phi}_k^{(\ell)})} s_{m,1} \tag{21}$$

is a weighted sum of the x-coordinates of devices associated with UAV k. Similarly, the update of y_k in iteration $\ell+1$ can be approximated as

$$y_k^{(\ell+1)} \approx (1-\alpha) y_k^{(\ell)} + \alpha \tilde{y}_k^{(\ell+1)}, \tag{22}$$

where

$$\tilde{y}_k^{(\ell+1)} \triangleq \sum_{m=1}^{M} \frac{a_{m,k} \tilde{\Psi}_m(\boldsymbol{\phi}_k^{(\ell)})}{\sum_{m'=1}^{M} a_{m',k} \tilde{\Psi}_{m'}(\boldsymbol{\phi}_k^{(\ell)})} s_{m,2}. \tag{23}$$

It is interesting to observe that, in iteration $\ell+1$, UAV k is moved horizontally towards the position $(\tilde{x}_k^{(\ell+1)}, \tilde{y}_k^{(\ell+1)})$, which is a weighted sum of the 2D coordinates of the associated devices. By observing more closely, we can see that the weights, i.e., $\{\tilde{\Psi}_m(\boldsymbol{\phi}_k^{(\ell)})\}_{m=1}^{M}$, are proportional to the load demands of the corresponding devices (i.e., $\{\lambda_m\}_{m=1}^{M}$). This implies that the UAV deployment policy should place more emphasis on devices with higher load demands. Hence, we refer to this algorithm as the iterative load-balancing (ILB) algorithm. Moreover, we can see that $\tilde{\Psi}_m(\boldsymbol{\phi}_k^{(\ell)})$ is positive if $\sqrt{(s_{m,1}-x_k)^2 + (s_{m,2}-y_k)^2} > r_k$ (i.e., if device m is outside the UAV's circular flight trajectory), and is negative, otherwise (i.e., if device m is inside the circular trajectory). In the former case, moving the trajectory center closer to device m reduces the transmission distance at the closest point, which is opposite in the latter case. This effect is unique to circling fixed-wing UAVs and is not captured by the K-means deployment often adopted in the literature.

In iteration $\ell+1$, the altitude and radius of UAV k can be updated by solving the optimization problem in (13) for fixed $(x_k, y_k) = (x_k^{(\ell+1)}, y_k^{(\ell+1)})$. In this case, we have

$$(h_k^{(\ell+1)}, r_k^{(\ell+1)}) = \underset{\substack{h_k \in [h_{\min}, h_{\max}] \\ r_k \in [r_{\min}, r_{\max}]}}{\arg\min} \sum_{m=1}^{K} a_{m,k} \lambda_{m,k} \tilde{\gamma}_{m,k}(x_k^{(\ell+1)}, y_k^{(\ell+1)}, h_k, r_k). \tag{24}$$

The optimization can be solved by a simple two-dimensional line search. The above procedures are repeated until no further improvement can be observed in the objective function. The algorithm is summarized in Algorithm 2

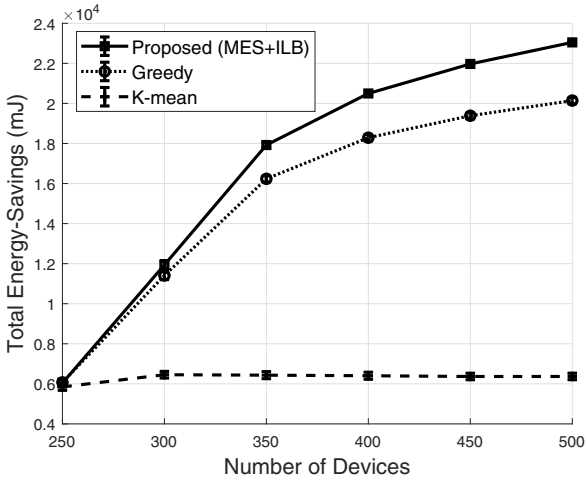

Fig. 2. Total energy-savings versus number of devices.

V. Simulation Results

In this section, we demonstrate the effectiveness of the proposed MES device association and the ILB UAV deployment and radius adjustment algorithms. In the experiments, IoT devices are deployed randomly according to a uniform distribution within a 600×600 m^2 area. For the LoS probability in (4), we consider an urban environment with $\psi = 11.95$ and $\beta = 0.14$ at 2 GHz carrier frequency. The period of the flight cycle is set as $T = 34$ seconds, and the minimum and maximum altitude of UAVs are $h_{\min} = 100$ and $h_{\max} = 300$ meters, respectively. The excessive path loss for LoS and NLoS are chosen as $\eta_{\text{LoS}} = 3$dB and $\eta_{\text{NLoS}} = 23$dB. The noise power is -82dBm, the SNR threshold is $\gamma_k = 10$ dB, for all k, and $P_{\max} = 30$mW. The altitude of all UAVs are initialized as $h_{\max}$ to ensure high coverage of ground devices.

The proposed MES device association algorithm is compared with two candidate algorithms namely, greedy and K-means algorithms. The greedy algorithm assigns devices to UAVs in the order of their potential energy savings, and is combined with our proposed ILB algorithm to determine the UAVs' trajectory centers and radii. The K-means algorithm places UAVs at the centroid positions of device clusters and associates devices to UAVs in the order of their distance to the centroid. The altitude and radius are optimized by (24). The load demand of devices (i.e., $\{\lambda_m\}_{m=1}^{M}$) are chosen randomly

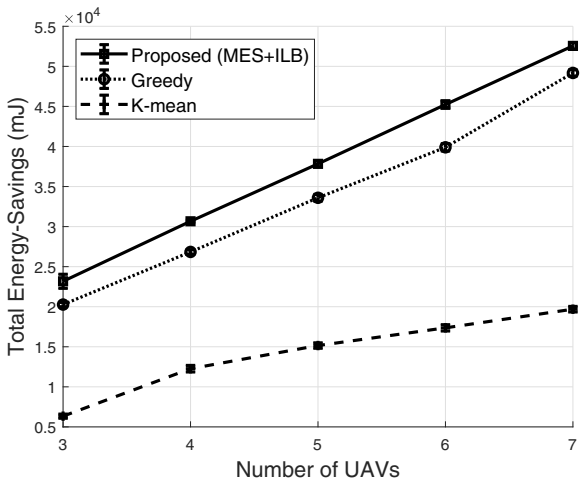

Fig. 3. Total energy-savings versus number of UAVs.

according to a uniform distribution between $[1, 10]$ units, and the capacity limits of the UAVs are set as $\mu_k = 500$ units, $\forall k$.

In Fig. 2, we show the total energy savings versus the number of IoT devices in the case with $K = 3$ UAVs. We can see that the total energy savings increases with the number of devices for both the proposed and the greedy algorithms whereas it remains relatively static for the K-means algorithm since the latter does not take into account the devices' power consumptions and demands in the association decisions. The advantage of our proposed scheme is most evident when the number of devices is large since, in this case, the capacity of UAVs becomes insufficient and, thus, proper device association becomes critical. The greedy approach is inferior to our proposed scheme since it does not take into account possible future assignments in each step of the algorithm.

In Fig. 3, we show the total energy savings versus the number of UAVs in the case with $M = 500$ devices. We can see that, as the number of UAVs increases, the energy-savings increases in all cases since more devices can be served and their distances to the associated UAVs are decreased. Our proposed scheme outperforms the greedy algorithm regardless of the number of UAVs, but the gain is reduced when the number of UAVs is large since, in this case, most sensors with considerable energy-savings can be served by both algorithms.

In Fig. 4, we show an example of the device association for cases where the number of UAVs is $K = 3$ and the number of devices is $M = 300$ and 380, respectively. We can see that the number of unassociated devices (i.e., black circle markers) increases as M increases. Notice that the unassociated devices may be located close to the trajectory centers since they are farther away from the circulating UAVs. This is contrary to rotary-wing UAVs that do not need to follow a circulating trajectory, but can stay at a static position.

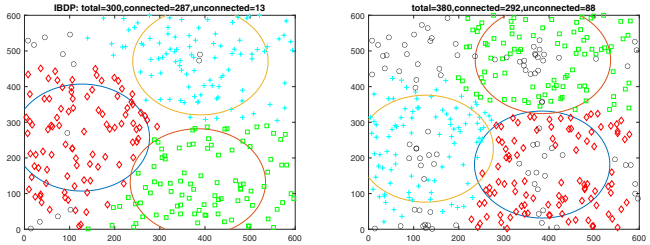

(a) $M = 300$ (b) $M = 380$

Fig. 4. Example of resulting device association and UAV deployment. Circle markers represent unassociated devices.

REFERENCES

[1] M. Mozaffari, W. Saad, M. Bennis, Y.-H. Nam, and M. Debbah, "A tutorial on UAVs for wireless networks: Applications, challenges, and open problems," *IEEE Commun. Surveys Tuts.*, vol. 21, no. 3, pp. 2334–2360, 2019.

[2] Y. Zeng, R. Zhang, and T. J. Lim, "Wireless communications with unmanned aerial vehicles: Opportunities and challenges," *IEEE Commun. Mag.*, vol. 54, no. 5, pp. 36–42, 2016.

[3] F. Cheng, S. Zhang, Z. Li, Y. Chen, N. Zhao, F. R. Yu, and V. C. M. Leung, "UAV trajectory optimization for data offloading at the edge of multiple cells," *IEEE Trans. Veh. Technol.*, vol. 67, no. 7, pp. 6732–6736, July 2018.

[4] M. Erdelj, E. Natalizio, K. R. Chowdhury, and I. F. Akyildiz, "Help from the sky: Leveraging UAVs for disaster management," *IEEE Pervasive Comput.*, vol. 16, no. 1, pp. 24–32, Jan 2017.

[5] Y. Zeng, R. Zhang, and T. J. Lim, "Throughput maximization for UAV-enabled mobile relaying systems," *IEEE Trans. Commun.*, vol. 64, no. 12, pp. 4983–4996, 2016.

[6] P. Zhan, K. Yu, and A. L. Swindlehurst, "Wireless relay communications with unmanned aerial vehicles: Performance and optimization," *IEEE Trans. Aerosp. Electron. Syst.*, vol. 47, no. 3, pp. 2068–2085, 2011.

[7] N. H. Motlagh, M. Bagaa, and T. Taleb, "UAV-based IoT platform: A crowd surveillance use case," *IEEE Commun. Mag.*, vol. 55, no. 2, pp. 128–134, 2017.

[8] N. H. Motlagh, T. Taleb, and O. Arouk, "Low-altitude unmanned aerial vehicles-based internet of things services: Comprehensive survey and future perspectives," *IEEE Internet Things J.*, vol. 3, no. 6, pp. 899–922, 2016.

[9] Y. Zeng and R. Zhang, "Energy-efficient UAV communication with trajectory optimization," *IEEE Trans. Wireless Commun.*, vol. 16, no. 6, pp. 3747–3760, 2017.

[10] C. Zhan, Y. Zeng, and R. Zhang, "Energy-efficient data collection in uav enabled wireless sensor network," *IEEE Wireless Commun. Lett.*, vol. 7, no. 3, pp. 328–331, June 2018.

[11] J. Gong, T. Chang, C. Shen, and X. Chen, "Flight time minimization of uav for data collection over wireless sensor networks," *IEEE J. Sel. Areas Commun.*, vol. 36, no. 9, pp. 1942–1954, Sep. 2018.

[12] M. Mozaffari, W. Saad, M. Bennis, and M. Debbah, "Mobile unmanned aerial vehicles (UAVs) for energy-efficient internet of things communications," *IEEE Trans. Wireless Commun.*, vol. 16, no. 11, pp. 7574–7589, 2017.

[13] ——, "Wireless communication using unmanned aerial vehicles (UAVs): Optimal transport theory for hover time optimization," *IEEE Trans. Wireless Commun.*, vol. 16, no. 12, pp. 8052–8066, 2017.

[14] K.-M. Chen, T.-H. Chang, and T.-S. Lee, "Lifetime maximization for uplink transmission in UAV-enabled wireless networks," in *Proceedings of IEEE International Conference on Wireless Communications and Networking Conference (WCNC)*, 2019.

[15] M. Dawande, J. Kalagnanam, P. Keskinocak, F. S. Salman, and R. Ravi, "Approximation algorithms for the multiple knapsack problem with assignment restrictions," *Journal of Combinatorial Optimization*, vol. 4, no. 2, pp. 171–186, 2000.

[16] S. Martello, *Knapsack problems: algorithms and computer implementations*, ser. Wiley-Interscience series in discrete mathematics and optimization. John Wiley & Sons Ltd., 1990.

[17] R.-H. Cheng, Y. P. Hong, and J.-P. Sheu, "Power efficient temporal routing and trajectory adjustment for multi-UAV networks," in *Proceedings of IEEE International Conference on Communications (ICC)*, 2019.

[18] A. Al-Hourani, S. Kandeepan, and S. Lardner, "Optimal LAP altitude for maximum coverage," *IEEE Wireless Commun. Lett.*, vol. 3, no. 6, pp. 569–572, 2014.